# Synthesis and evaluation of $Fe_3O_4$-impregnated activated carbon for dioxin removal

Yao-Jen Tu[a], Gnanasiri S. Premachandra[b], Stephen A. Boyd[c], J. Brett Sallach[d], Hui Li[c], Brian J. Teppen[c], Cliff T. Johnston[b,e*]

[a] School of Environmental and Geographical Sciences, Shanghai Normal University, 100 Guilin Rd. Shanghai, 200234, China

[b] Department of Agronomy, Purdue University, 915 W. State Street, West Lafayette, Indiana 47907, USA

[c] Department of Plant, Soil, and Microbial Sciences, Michigan State University, East Lansing, Michigan, 48824, USA

[d] Department of Environment and Geography, University of York, Heslington, York, YO10 5NG, UK

[e] Department of Earth, Atmospheric and Planetary Sciences, 550 Stadium Mall, Purdue University, West Lafayette, IN 47907, USA

Corresponding author: Cliff T. Johnston

Fax: +1-7654961716

E-mail: cliffjohnston@purdue.edu

1    Synthesis and evaluation of $Fe_3O_4$-impregnated activated carbon for dioxin removal

2

3    Yao-Jen Tu[a], Gnanasiri S. Premachandra[b], Stephen A. Boyd[c], J. Brett Sallach[d], Hui Li[c], Brian

4    J. Teppen[c], Cliff T. Johnston[b,e*]

5

6    [a] School of Environmental and Geographical Sciences, Shanghai Normal University, 100

7    Guilin Rd. Shanghai, 200234, China

8    [b] Department of Agronomy, Purdue University, 915 W. State Street, West Lafayette, Indiana

9    47907, USA

10    [c] Department of Plant, Soil, and Microbial Sciences, Michigan State University, East Lansing,

11    Michigan, 48824, USA

12    [d] Department of Environment and Geography, University of York, Heslington, York, YO10

13    5NG, UK

14    [e] Department of Earth, Atmospheric and Planetary Sciences, 550 Stadium Mall, Purdue

15    University, West Lafayette, IN 47907, USA

16    Corresponding author: Cliff T. Johnston

17        Fax: +1-7654961716

18        E-mail: cliffjohnston@purdue.edu

19

20  **Abstract**

21    Polychlorinated dibenzo-p-dioxins and -furans (PCDD/PCDFs) are highly toxic organic

22  pollutants in soils and sediments which persist over timescales that extend from decades to

23  centuries. There is a growing need to develop effective technologies for remediating

24  PCDD/Fs-contaminated soils and sediments to protect human and ecosystem health. The use

25  of sorbent amendments to sequester PCDD/Fs has emerged as one promising technology. A

26  synthesis method is described here to create a magnetic activated carbon composite

27  (AC-$Fe_3O_4$) for dioxin removal and sampling that could be recovered from soils using

28  magnetic separation. Six AC-$Fe_3O_4$ composites were evaluated (five granular ACs (GACs)

29  and one fine-textured powder AC(PAC)) for their magnetization and ability to sequester

30  dibenzo-p-dioxin (DD). Both GAC/PAC and GAC/PAC-$Fe_3O_4$ composites effectively

31  removed DD from aqueous solution. The sorption affinity of DD for GAC-$Fe_3O_4$ was slightly

32  reduced compared to GAC alone, which is attributed to the blocking of sorption sites. The

33  magnetization of a GAC-$Fe_3O_4$ composite reached 5.38 emu/g based on SQUID results,

34  allowing the adsorbent to be easily separated from aqueous solution using an external

35  magnetic field. Similarly, a fine-textured PAC-$Fe_3O_4$ composite was synthesized with a

36  magnetization of 9.3 emu/g.

37

38  Keywords: dibenzo-p-dioxin, granular activated carbon, $Fe_3O_4$, magnetic separation,

39    activated carbon-$Fe_3O_4$ composite

## 1. Introduction

41    Polychlorinated dibenzo-p-dioxins (PCDDs) are prototypical persistent organic pollutants

42    (POPs) that are commonly found in soils and sediments. Due to their exceptionally low water

43    solubilities, these highly toxic lipophilic substances are highly bio-accumulative (Guruge et

44    al., 2005; Maier et al., 2016; Champoux et al., 2017). Exposure to PCDDs, even at trace

45    concentrations (Denison et al., 1989; Eljarrat et al., 2002), can result in measurable toxic and

46    carcinogenic effects in mammals (Huwe, 2002; McKay, 2002; Charnley and Doull, 2005).

47    PCDDs occur both naturally and from anthropogenic activities which include forest fires,

48    coal combustion, iron ore sintering, chlorine bleaching of pulp and paper, waste incineration,

49    and as by-products of pesticide manufacturing and the chlor-alkali process (Fiedler, 1996;

50    Everaert and Baeyens, 2002; Kulkarni et al., 2008; Zheng et al., 2008; Zhou et al., 2016;

51    Prisciandaroa et al., 2017; Zhao et al., 2017). Owing to their lipophilicity, PCDD/Fs

52    accumulate in surface soils, sediments and biota, including the fatty tissues of fish (WHO,

53    2010). In natural environments, they occur predominantly in the sorbed state associated with

54    pyrogenic carbonaceous matter (PCM), amorphous organic matter, and clays (Ferrario et al.,

55    2000; Fabietti et al., 2010). In fact, the significant role of PCM as a sorption domain has been

56    well established (Cornelissen et al., 2005). As a group, PCDD/Fs are characterized by low

57    aqueous solubilities and high octanol-water coefficients $K_{ow}$ (Shiu et al., 1988; Kim et al.,

58 2002; Li et al., 2009). Consequently, their concentrations in natural waters are extremely low

59 with concentration ranges of pg/L to fg/L (Charlestra et al., 2008; Cornelissen et al., 2008b;

60 Louchouarn et al., 2018). PCDD/F-contaminated soils are found in ecosystems worldwide

61 (Masunaga et al., 2001; Moon et al., 2008; Zheng et al., 2008), and have proven difficult and

62 expensive to remediate. For example, the estimated cleanup cost of a *single* Superfund site

63 along the Passaic River which is contaminated by PCDD/Fs has exceeded one billion US

64 dollars.

65     Traditional site remediation has relied on removal of the contaminants via excavation or

66 dredging followed by disposal in a hazardous waste landfill. Recently, sorbent amendments

67 have gained attention as a means to lower or even eliminate bioavailability of soil/sediment-

68 bound contaminants (Ghosh et al., 2011; Cornelissen et al., 2012; Hale et al., 2012;

69 Cornelissen et al., 2016; Cho et al., 2017), and this has formed the basis of a new direction in

70 management of sites contaminated with PCDD/Fs (Ghosh et al., 2011). Activated carbon

71 (AC) materials (including granular activated carbon (GAC) and powdered activated carbon

72 (PAC), has emerged as an effective sorbent amendment for this purpose (Cornelissen et al.,

73 2012; Denyes et al., 2013; Gomez-Eyles et al., 2013; Balasubramani and Rifai, 2018).

74     The retrieval of the amendment with its sorbed contaminants after deployment has

75 become a priority for a number of reasons. First, complete removal of contaminants, rather

76 than just immobilization, is preferred by many environmental regulatory agencies (e.g.,

77  USEPA, 1997). Second, recovery of the sorbent amendment after its use as a passive sampler

78  can help determine mass transfer kinetics (Cornelissen et al., 2008a; Oen et al., 2011).

79  Adsorbent magnetization is an emerging remediation area where magnetic separation

80  simplifies isolation and regeneration (Mohan et al., 2014). Numerous studies have

81  demonstrated that activated carbon/$Fe_3O_4$ composites can be synthesized that maintain high

82  surface area and high sorption affinities for a growing list of contaminants that includes

83  organic dyes (Do et al., 2011), arsenic (Zhang et al., 2007, Zhang et al., 2010), heavy metals

84  (Han et al., 2015), pesticides and PAHs (Mohan et al., 2014).   Our previous work showed

85  that magnetic $Fe_3O_4$ can be easily fabricated from the hydrothermal ferrite process and has

86  the potential to remove/recover toxic/precious elements from aqueous solutions (Tu et al.,

87  2012; Tu et al., 2013; Tu et al., 2015). To date, adsorbent magnetization has not been applied

88  to applications involving PCDD/Fs.

89      In our prior work, we provided the first evidence that bioavailability of TCDD sorbed to

90  two contrasting GACs and one PAC was eliminated in the mammalian (mouse) model. This

91  conclusion was based upon the use of two highly sensitive bioassays, hepatic induction of

92  cyp1A1 mRNA, an indirect measure of TCDD exposure, and immunoglobulin M antibody-

93  forming cell response, a direct measure of immune response (Boyd et al., 2017; Sallach et al.,

94  2019). Prior to this, reductions in bioavailability had only been established based on simpler

95  model organisms (e.g., worms) or passive samplers (Fagervold et al., 2010; Chai et al., 2011;

5

96    Chai et al., 2012). Although the ACs represented a wide range of particle size and pore size

97    distributions, they were equally effective in eliminating the bioavailability of TCDD, making

98    them viable candidates for remediation. In this study, we pursued an additional line of

99    investigation to determine if these same ACs could be functionalized using *in situ* synthesis

100   of $Fe_3O_4$ for subsequent magnetic retrieval (Indhu et al., 2015; Choi et al., 2016) without

101   compromising their affinity for dioxins.

102      AC-$Fe_3O_4$ composites were synthesized using the same GACs/PAC used in prior

103   bioavailability studies (Boyd et al., 2017; Sallach et al., 2019). The specific goals of the

104   current work were to (1) synthesize GAC/PAC-$Fe_3O_4$ composites using ACs shown to be

105   effective in eliminating TCDD bioavailability in mammals, with emphasis on gaining new

106   physicochemical insight into the interaction between GAC/PAC and $Fe_3O_4$, (2) characterize

107   the composites using a combination of X-ray diffraction (XRD), scanning electron

108   microscopy (SEM), $N_2$-BET and micropore analysis, and superconducting quantum

109   interference device (SQUID); and (3) evaluate sorption characteristics (kinetics and

110   equilibration) of GAC/PAC, $Fe_3O_4$, and the GAC/PAC-$Fe_3O_4$ composite for aqueous phase

111   dibenzo-p-dioxin (DD). The compound DD served as an isostructural conservative surrogate

112   for PCDD/Fs, which are important targets for sequestration using environmental geosorbents

113   due to their extreme recalcitrance in natural environments (Van Den Berg et al., 1998;

114   Sallach et al., 2019; Johnston et al., 2012).
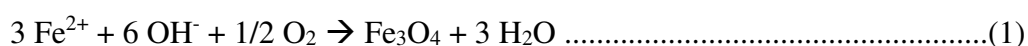
## 2. Materials and methods

2.1. Chemicals and materials

All solutions were prepared with deionized water. $Fe_3O_4$ was synthesized from ferrous

sulfate $FeSO_4$ (> 99.9%, Fisher Scientific, USA) and sodium hydroxide NaOH (99.5%,

Fisher Scientific, USA). Dibenzo-p-dioxin (99% pure) was purchased from ChemService

(West Chester, PA, USA) and was used as received. All the reagents are of analytical grade

and used without further purification. Five GACs (DSRA, G60, FM-1, TOG-LF, and, F400)

and one fine textured PAC (WPC) were purchased/obtained from USEPA, Sigma Aldrich,

Cabot, Calgon Carbon Corp,. Selected physical properties of the six GACs/PAC are given in

Table 1.

2.2. Synthesis procedure for magnetic AC-$Fe_3O_4$ composites

The magnetic GAC/PAC-$Fe_3O_4$ composite synthesis followed two synthesis procedures

modified from our previously published method (Tu et al., 2013). Method A was performed

using 0.01 M $FeSO_4$ at T=338 K, pH 10, and a reaction time of 2 h. Method B was carried

out using 0.1 M $FeSO_4$ at T=298 K, pH 10, and the same 2 h reaction time. Briefly, one gram

of GAC/PAC material was dried under vacuum at room temperature for 20 h using a vacuum

oven (Model 280 A, Fisher Scientific, USA). Dried GAC/PAC was then immersed in 0.01 M

(Method A) or 0.1 M (Method B) $FeSO_4$ solution (0.5 L) and mixed continuously at room

temperature for 20 h. After mixing, the pH was adjusted to 10 by dropwise addition of 0.1 M

134    NaOH and then air was bubbled to the solution to initiate the reaction. The synthesis

135    reactions were carried out at 338 K (Method A) or 298 K (Method B) for 2 h while

136    maintaining the pH at 10. Finally, the resultant AC-$Fe_3O_4$ material was rinsed 5x with DI

137    water to remove free $Fe_3O_4$, and successfully magnetized GAC/PAC-$Fe_3O_4$ composites was

138    separated from the solution via magnet. The corresponding synthetic reaction of $Fe_3O_4$ can be

139    described as Eq. 1 (Tu et al., 2013).

140    $3\ Fe^{2+} + 6\ OH^- + 1/2\ O_2 \rightarrow Fe_3O_4 + 3\ H_2O$ .......................................................(1)

141    2.3. Characterization of AC-$Fe_3O_4$ composite

142    The crystal phases were determined by X-ray diffraction (XRD; X'Pert Pro, Philips,

143    Netherlands) using graphite monochromatic cobalt radiation over the 2θ range 10-80°. The

144    surface morphology and particle size were examined by scanning electron microscopy (SEM;

145    Nova NanoSEM, Oxford instruments, UK). The saturation magnetization of the adsorbent

146    was measured using a Superconducting Quantum Interference Device (SQUID

147    magnetometer; MPMS-3, Quantum Design, USA) at 300 ±1 K. $N_2$ BET and micropore

148    analysis was conducted using a Micromeritics 3Flex Multiport Chemi/Physi/Micropore

149    Analyzer.

150    2.4. Measurement of adsorption isotherm

151    Batch adsorption experiments were conducted in duplicate using five initial aqueous DD

152    concentrations (0.18, 0.3, 0.4, 0.6 and 0.8 mg/L) prepared by a serial dilution of 800 mg/L of

153    DD methanol stock solution. The amount of methanol in the aqueous solutions was 0.1%

154    which is considered to have minimal cosolvent effects. Aqueous solutions of DD were

155    sonicated for 60 min at room temperature in a water bath sonicator prior to mixing with the

156    GAC/PAC (Branson 120, Branson Ultrasonics, Danbury, CT, USA).

157        Two and half (2.5) mg of the adsorbent (GAC, PAC, GAC-$Fe_3O_4$, PAC-$Fe_3O_4$) was

158    placed in 30 mL Corex glass tubes (Kimble, Vineland, NJ, USA) with

159    polytetrafluoroethylene (PTFE)-lined screw caps, and mixed with a 30 mL aliquot of DD in

160    aqueous solutions (methanol 0.1 %). Control samples containing the initial aqueous DD

161    solutions 0.6 and 0.8 mg/L of DD solution without AC were prepared for calibration to

162    determine the losses of DD in the batch reactor. Measured values of DD in the control

163    samples ranged from 0.58 to 0.62 mg/L and 0.78 to 0.82 mg/L for the 0.6 and 0.8 mg/L DD

164    solutions, respectively. These results indicated that loss of DD to glassware can be ignored.

165    The suspensions were sonicated for 30 sec prior to shaking at a speed of 60 rpm in a rotary

166    shaker (Glas-Col, Terre Haute, IN, USA) at room temperature for 10-48 h to achieve the

167    apparent sorption equilibrium. The supernatant and adsorbent were separated by

168    centrifugation for GAC/PAC and by external magnetic field for GAC/PAC-$Fe_3O_4$

169    composites. An aliquot of 1.0 mL of supernatant and DD standards (0.0, 0.18, 0.3, 0.4, 0.6

170    and 0.8 mg/L) were transferred to HPLC vials. In order to prevent any sorption of DD by

171    HPLC vials, 0.5 mL of methanol (99.9%) was added to each vial prior to the addition of the

172    supernatant. HPLC vials containing supernatant and methanol were vortexed for 30 sec using

173    a digital mini-vortexer (VWR, Radnor, PA, USA). Samples were then analyzed for DD

174    concentrations by direct injection of 50 μL into a Thermo Scientific high-performance liquid

175    chromatography (HPLC) system (Ultimate 3000) equipped with a UV detector and a 150×

176    4.60 mm 5 micron Luna 5 μm C8(2) 100 Å column (S/N 514816-4). Isocratic elution was

177    performed using a mobile phase of 80% methanol: 20% water (v/v) with a flow rate of 1.0

178    mL/min and wavelength of 223 nm for detection.

179        The amount of DD sorbed ($q_e$, mg/kg) was calculated as the difference between the

180    amount initially added and that remaining in the solution after equilibration (Eq. 2):

181    $$q_e = \frac{(C_o - C_e) \times V}{m_{ads}} \dots\dots\dots\dots\dots\dots\dots\dots\dots\dots\dots\dots\dots\dots\dots\dots\dots\dots\dots\dots\dots(2)$$

182    where $C_o$ and $C_e$ are DD concentration in liquid phase at time zero and after equilibration

183    (mg/L), respectively; V is the solution volume used in DD adsorption (L); $m_{ads}$ is GAC/PAC

184    mass (kg).

185    2.5. Desorption

186        Following collection of the supernatant after equilibrium had been reached, the remaining

187    supernatant was carefully decanted and the solid phase was re-suspended in a 30 mL solution

188    of 25% and 99.9% methanol and water (v/v). Tubes were sonicated for 30 sec prior to

189    shaking 24 h at 60 rpm to ensure equilibrium. Then, the supernatant and adsorbent were

190    separated by either centrifugation (GAC/PAC) or external magnetic field (GAC/PAC-$Fe_3O_4$

10

191    composite). Approximately 1.5 mL aliquots of supernatant and standards of 0.18, 0.3, 0.4, 0.6

192    and 0.8 mg/L were transferred to HPLC vials for HPLC analysis. The amount of DD

193    desorbed was calculated directly from the concentration of DD present in the supernatant

194    following equation Eq. 3:

195    Desorption efficiency $= \dfrac{C \times V}{X} \times 100\%$…………………………………......(3)

196    where C (mg/L) is the concentration of DD in the desorption solution, V (L) is the volume of

197    the desorption solution, and X (g) is the amount of DD adsorbed.

198

199    **3.  Results and discussion**

200    3.1. Adsorbent characterization in GAC

201        Six activated carbon materials consisting of five granular activated carbon (GAC)

202    materials (F400, FM-1, G60, TOG-LF, and DSRA) and one fine textured powdered activated

203    carbon powder (PAC) (WPC) were functionalized with $Fe_3O_4$. Selected physical properties of

204    the six materials are given in Table 1.   All but one of these GAC/PAC materials (DSRA)

205    were used in recent TCDD bioavailability studies and were found to be highly effective in

206    eliminating mammalian bioavailability of TCDD (Boyd et al., 2017; Sallach et al., 2019).

207        The activated carbon materials (Table 1) were functionalized using two different

208    magnetite synthesis methods. Given their large specific surface areas and micropore (0-2 nm

209    pores) volumes (Table 1), some magnetite synthesis was expected to occur in the micro- and

210     mesopores (2-50 nm pores) of the GAC/PAC, along with surface decoration of exterior

211     surfaces of the GAC/PAC particles rendering the GAC/PAC-$Fe_3O_4$ composites magnetic.

212     $Fe_3O_4$ synthesis Method A was performed at elevated temperature (338 K) using 0.01 M

213     $FeSO_4$. The resulting magnetization of the PAC-$Fe_3O_4$ composite was successful with a value

214     of 9.7 emu/g (Table 1). In contract, observed magnetization values measured at 300 K for the

215     five GACs were weak with values of 0.61 (DSRA), 0.54 (FM-1), 0.49 (TOG-LF), 0.46 (G60)

216     and 0.35 (F-400) emu/g (Table 1). For comparison, the magnetization of $Fe_3O_4$ synthesized

217     using Synthesis Method A without GAC/PAC was 71.9 emu/g.   Weak magnetization values

218     in the ranged of 0.35-0.61 emu/g were not sufficient to allow rapid magnetic separation.

219         Because the magnetization values resulting from synthesis Method A for the granular

220     activated carbon samples were weak (0.35-0.61 emu/g), the $Fe_3O_4$ synthesis procedure was

221     modified using synthesis Method B, which utilized a higher concentration of $FeSO_4$ (0.1 M)

222     and a lower temperature of 298 K. The granular activated carbon sample DSRA was selected

223     because it showed the highest level of magnetization among the five GAC materials

224     evaluated using Method A (Table 1). Synthesis Method B resulted in a DSRA-$Fe_3O_4$

225     composite with a significantly improved magnetization value of 5.38 emu/g (Table 1). No

226     residual magnetism was detected in either of the GAC(DSRA)-$Fe_3O_4$ (Synthesis Method B)

227     or PAC(WPC)/$Fe_3O_4$ (Synthesis Method A) composites indicating that these two materials

228     are superparamagnetic (Table 1). For simplicity, the GAC(DSRA)-$Fe_3O_4$ complex (using

229    Synthesis Method B) will be referred to as GAC-Fe$_3$O$_4$(B) and the PAC(WPC)-Fe$_3$O$_4$

230    complex (using Synthesis Method A) will be referred to as PAC-Fe$_3$O$_4$(A), where (A) and

231    (B) refer to Synthesis Methods A and B, respectively.

232    The GAC-Fe$_3$O$_4$(B) composite in aqueous suspension was efficiently recovered by

233    applying an external magnetic field. The complete (~100%) separation of the GAC-Fe$_3$O$_4$(B)

234    composite from solution using a magnet was achieved within only 20 seconds (Supplemental

235    Information Fig. S1). When the external magnetic field was removed, the GAC-Fe$_3$O$_4$(B)

236    composite could be readily dispersed again in water by physical shaking.

237    The XRD patterns of the GAC-Fe$_3$O$_4$(B) and PAC-Fe$_3$O$_4$(A) composites are shown in

238    Fig. 2. The observed diffraction peaks at d-spacings of 4.846, 2.968, 2.531, 2.423, 2.099,

239    1.713, 1.615, and 1.484 Å matched the XRD reflections of Fe$_3$O$_4$ (JCPDS file number 04-

240    007-9093). No other peaks were detected in the XRD pattern of the GAC-Fe$_3$O$_4$(B)

241    confirming that the only crystalline phase present is Fe$_3$O$_4$ nanoparticles in the GAC-

242    Fe$_3$O$_4$(B) composite. In addition to the Fe$_3$O$_4$ peaks, the PAC-Fe$_3$O$_4$(A) composite had small

243    peaks at 24.2, 31.0 and 58.5 °2θ.

244    Further characterization of the GAC and the GAC-Fe$_3$O$_4$(B) composite was provided by

245    SEM imaging of the two materials at different levels of magnification (Figs. 3a-3f). The

246    average bulk size of the GAC was ~1 mm with <5% passing through a 40 US Mesh sieve

247    (420 µm) (Fig. 3a); 'large' pores were observed ranging in size from several µm to >10 µm

248 (Figs. 3b and 3c). The synthesized $Fe_3O_4$ particles were observed to be spherical, and their

249 primary particle size ranged between 20 and 120 nm (Fig. 3d). From the SEM images it is

250 evident that the synthesized $Fe_3O_4$ nanoparticles were randomly distributed on the surfaces

251 and pores of the GAC particles (Fig. 3f).

252     3.2  $N_2$ BET and Textural Analysis

253     $N_2$ BET and micro-textural analysis of the activated carbon materials prior to magnetite

254 synthesis are presented in Table 1. The supplier of the activated carbon, feedstock, along with

255 $N_2$ BET surface area and micropore analysis are presented in Table 1. The five granular

256 activated carbon samples ranged in percentage micropore (0-2 nm) volume from 29 to 82%

257 of the total micropore and mesopore (2-50 nm) volume.   The fine textured WPC powder had

258 very little mesoporosity with 91% of its pore volume in the micropore range.   Of the six

259 samples, five were used in prior toxicology studies to assess TCDD bioavailability (Boyd et

260 al., 2017; Sallach et al., 2019). Although these ACs represented a wide range of particle size

261 and pore size distributions, they were equally effective in eliminating the bioavailability of

262 TCDD, making them viable candidates for remediation. After $Fe_3O_4$ synthesis, the specific

263 surface area of the GAC(DSRA)-$Fe_3O_4$ composite decreased from 822 to 633 $m^2/g$ along

264 with a modest reduction in micropore volume (0.388 to 0.262 g/cc) indicative of some partial

265 pore blocking by the magnetite particles (Table 1).

266    3.3. Batch equilibrium sorption and kinetics

267        Batch sorption isotherms of dibenzo-p-dioxin (DD) to GAC and GAC-Fe$_3$O$_4$(B) are

268    shown in Fig. 4. Both GAC and GAC-Fe$_3$O$_4$ composite showed a high affinity for aqueous

269    phase DD at low equilibrium concentrations (<0.005 mg/L) up to a sorbed concentration

270    about of about 4000 mg/kg. At higher equilibrium concentrations (0.005-0.12 mg/L), sorption

271    isotherms showed some nonlinear behavior exhibiting high affinity at low equilibrium

272    concentration followed by an "S-shaped" response (Giles and Smith, 1974). The GAC-

273    Fe$_3$O$_4$(B) isotherm is shifted to higher equilibrium concentrations (i.e., lower affinity)

274    compared the GAC, however, both materials sorbed > 8000 mg/kg. These results could be

275    explained by sorption processes involving easily accessible external sites and less accessible

276    pores. Since Fe$_3$O$_4$ demonstrated no sorption affinity for DD, its presence within the GAC

277    composite likely blocked some sorption sites or access to certain pores manifesting a slight

278    decrease in DD affinity.

279        The kinetics of DD sorption by GAC and GAC-Fe$_3$O$_4$ composite were evaluated over a

280    period of 40 h using the batch equilibration method (described above) with initial aqueous

281    phase DD concentrations of 0.18, 0.4, and 0.8 mg/L (Fig. 5). Sorption kinetics of DD can be

282    separated into two phases. Initially, within the first 10 h, both GAC and GAC-Fe$_3$O$_4$

283    demonstrated comparatively rapid uptake of DD for all three initial concentrations. This was

284    followed by a slower phase (>50 h) to reach apparent equilibrium.

15

285     For the lower and intermediate initial DD concentrations of 0.18 and 0.4 mg/L, DD

286     uptake from aqueous solution by GAC was rapid and nearly complete within the first 10 h;

287     the percent DD removal approached 100 percent (Fig 5c-f). However, at the higher initial DD

288     concentration of 0.8 mg/L, there is a more gradual approach to apparent equilibrium over

289     time (Fig. 5a-b). For the initial concentrations of 0.18 and 0.4 mg/L, DD adsorption by GAC

290     was essentially complete by 10 h, and the total uptake of DD from aqueous solution

291     approached 100 percent. For the initial concentration of 0.8 mg/L the data indicate that

292     equilibrium had not been achieved after 50 h for GAC-$Fe_3O_4$.

293     For this system, it is assumed that sorption kinetics are controlled surface adsorption with

294     associated resistance to film diffusion followed by an emerging contribution to DD sorption

295     via intraparticle diffusion. Pseudo-second order kinetic models are commonly used to

296     describe sorption kinetics for these types of interactions (Ho and, McKay, 1999;

297     Amarasinghe and Williams, 2007).    The pseudo-second order kinetic model was able to fit

298     the experimental data well (see Table 2).    The pseudo-second order model results are plotted

299     on the kinetics data shown in Fig. 5.

300     The correlation coefficients ($R^2$) and kinetic parameters derived from the pseudo-second

301     order models are summarized in Table 2. These results suggest that the rate-limiting step may

302     be some type of site-specific mechanism involving direct interaction between the sorbent and

303     sorbate (Amarasinghe and Williams, 2007). The kinetic rate constant ($k_2$) from the pseudo-

304     second order model decreased with increasing initial DD concentrations (Table 1), indicating

305     that the DD adsorption rates are faster at lower concentrations. In other words, the time

306     required to reach equilibrium increased as the initial DD concentration increased. This is

307     likely due to competition for active surface sites and pores of the sorbent which is greater at a

308     higher DD concentration.

309     3.4 Desorption of DD

310         Desorption of DD into solutions of either 25% or 99.9% methanol and water (v/v)

311     desorption solutions were used to evaluate the reversibility of DD sequestration by GAC and

312     the GAC-$Fe_3O_4$ composite. Desorption of DD from GAC and GAC-$Fe_3O_4$ in 99.9% methanol

313     was 19% and 14.3% (after 20 h), respectively, and 11.2% and 12.4% for 25%

314     methanol/water, respectively.    These results agree with our prior study that showed 22-27%

315     of TCDD bound to three of the activated carbons samples used in the present study could be

316     desorbed after 64 hours of Soxhlet extraction using toluene (Sallach et et., 2019).

317     Magnetizing GAC with $Fe_3O_4$ had little to no effect on the propensity of DD to desorb. That

318     the fraction of released DD was less than 20% even for 99.9% methanol clearly indicated the

319     strong affinity between DD and GAC; once sorbed DD appears to be largely irreversibly-

320     sequestered within the pore structure of GAC. The resistance to desorption, even into

321     methanol, is consistent with our prior observation that sequestration of 2,3,7,8-TCDD by AC

322     eliminated its mammalian bioavailability (Boyd et al., 2017; Stedtfeld et al., 2017).

323  3.5 Sorption removal comparison of fine-textured AC-Fe$_3$O$_4$ to GAC-Fe$_3$O$_4$

324     The uptake of DD by GAC, GAC-DSR-Fe$_3$O$_4$(B), PAC and PAC-Fe$_3$O$_4$(A) as a function

325  of time are shown in Fig. 6. As expected, uptake of DD by the fine-textured AC (WPC) was

326  rapid and nearly stoichiometric. More than 90% of the WPC has a particle size of < 45 μm

327  (Sallach et al., 2019). In contrast, sorption kinetics for DD uptake by the coarse-textured

328  GAC and GAC-Fe$_3$O$_4$(B) were considerably slower. Although the surface area of the PAC,

329  GAC and their Fe$_3$O$_4$ derivatives are comparable, most of the surface area in GAC can only

330  be accessed through intraparticle diffusion, resulting in slower sorption kinetics (Figs. 5-6).

331  **4.  Discussion**

332     The activated carbon materials, including GAC and PAC, used here to form the magnetic

333  variants were also used in our prior bioavailability studies (Boyd et al., 2017; Stedtfeld et al.,

334  2017; Sallach et al., 2019), along with natural geosorbents including clay minerals and silica

335  (Boyd et al., 2011; Kaplan et al., 2011; Chai et al., 2016). Among these, only GAC and PAC

336  eliminated the bioavailability of sorbed TCDD to a mammalian (mouse) model.

337  Mammalian bioavailability was evaluated in our prior work using two highly sensitive

338  bioassays, hepatic induction of cyp1A1 mRNA, an indirect measure of TCDD exposure, and

339  immunoglobulin M antibody-forming cell response, a direct measure of immune response

340  (Boyd et al., 2017; Sallach et al., 2019).   In contrast to the complete elimination of TCDD

341  bioavailability achieved via sequestration by GAC/PAC, TCDD bound to clay minerals and

18

342  silica was found to be 100% bioavailable. The lack of mammalian bioavailability of TCDD

343  bound to GAC/PACs was consistent with a related study showing contaminant bioavailability

344  to lower organisms was significantly decreased in the presence of AC (Chai et al., 2012). In

345  addition, attempts to extract sorbed TCDD from ACs using Soxhlet extraction revealed that

346  only a minor fraction of the total TCDD present could be recovered (Sallach et al., 2019).

347  From an applied perspective, these laboratory results are now leading to the use of GAC/PAC

348  sorbent amendments in large-scale remediation efforts for impacted soils, sediments and

349  water bodies (Samuelsson et al., 2017; Payne et al., 2019; Cornelissen et al., 2016;

350  Beckingham et al., 2011). Given our earlier results showing elimination of mammalian

351  TCDD bioavailability, creating magnetic GAC/PAC composites that could be used as a

352  retrievable form of GAC/PAC sorbent amendments was attempted. The ability to retrieve

353  magnetized GAC/PAC would enhance their utility as passive samplers in field settings and in

354  ongoing laboratory studies. For example, our earlier mammalian studies would have

355  benefited from using a magnetic AC to determine the amount TCDD in fecal pellets from

356  mice that were dosed with TCDD–AC (Boyd et al., 2017; Stedfeldt et al., 2017; Sallach et al.,

357  2018). Likewise, the ability to ultimately retrieve (magnetized) GAC/PAC sorbent

358  amendments used to remediate areas with especially high levels of contamination would

359  provide both an immediate benefit, i.e., bioavailability reduction, and make contaminant

360  removal possible in the longer term.

361    The synthesis procedure using a lower concentration of $FeSO_4$ (0.01 M) at an elevated

362    temperature (338 K), Synthesis Method A, was successful in synthesizing a magnetic PAC-

363    $Fe_3O_4$ composite (PAC-$Fe_3O_4$(A)).    In the case of the PAC, magnetization most likely

364    occurs on the external surfaces of fine-textured AC and this could be accomplished using the

365    lower concentration of $FeSO_4$. However, Method A only produced weak magnetization

366    values for the GAC-$Fe_3O_4$ composites.    One could argue that this procedure was not able to

367    synthesize $Fe_3O_4$ particles within the coarse textured GACs. The procedure was modified

368    using a higher concentration of $FeSO_4$ (0.1 M) and lower temperature that resulted in a

369    sufficiently magnetic GAC-$Fe_3O_4$(B) composite.

370    Both the GAC-$Fe_3O_4$(B) and PAC-$Fe_3O_4$(A) composites revealed the presence of $Fe_3O_4$

371    based on X-ray diffraction analysis (Fig. 2) and it is possible that careful XRD studies could

372    be used as a surrogate for the more difficult to obtain SQUID magnetization results. $N_2$ BET

373    surface area and textural analysis showed that both the GAC and PAC materials were

374    characterized by high $N_2$-surface area (802-822 $m^2/g$).    The specific surface area of the

375    GAC-$Fe_3O_4$(B) composite showed a modest reduction in both surface area (822 to 633 $m^2/g$)

376    and micropore volume (0.38 g/cc to 0.26 g/cc) compared to the starting GAC (Table 1).

377    The batch sorption isotherms of dibenzo-p-dioxin (DD) on the GAC and GAC-$Fe_3O_4$(B)

378    composites showed that sorption affinity of DD was slightly reduced due to the presence of

379    magnetite particles (GAC-$Fe_3O_4$(B)) compared GAC. The decrease in surface area and DD

20

380    sorption is interpreted as some blocking of pore throats. Overall, the sorption isotherms for

381    both GAC and GAC-Fe$_3$O$_4$(B) showed some sorption nonlinearity, consistent with a range of

382    sorption sites of varying accessibility.

383        The sorption kinetics of DD uptake by GAC, GAC-Fe$_3$O$_4$(B), PAC and PAC-Fe$_3$O$_4$(A)

384    were strongly dependent on particle size. Uptake of DD by the fine textured PAC and PAC-

385    Fe$_3$O$_4$(A) composite was rapid and complete within 10 hours.    In contrast, sorption uptake

386    was much slower for GAC and the GAC-Fe$_3$O$_4$(B) composite (Fig. 4 and 5) owing to the

387    larger particle size.    Sorption equilibria had not been reached for the GAC-Fe$_3$O$_4$(B)

388    composite after 40 h. These results are consistent with prior work showing the influence of

389    particle size on sorption kinetics of hydrophobic organic solutes on activated carbon and

390    biochars (Ahn et al., 2005; Kang et al., 2018). As shown, the rate of DD uptake by the fine

391    textured AC and AC-Fe$_3$O$_4$(A) is rapid with showing 97% removal of DD from aqueous

392    solution after one hour. The larger sized GAC, with particle diameters ~ 1 mm (5% < 420

393    μm), showed much slower uptake (Fig. 6a) and is attributed to the longer diffusion pathways

394    to binding sites and pore structures in GAC.

395        We demonstrated that both a GAC and a PAC could be magnetized and, more

396    importantly, the GAC-Fe$_3$O$_4$(B) and PAC-Fe$_3$O$_4$(A) composites maintained high sorption

397    affinity for dioxin.    Particle size was a dominant factor in controlling sorption kinetics, with

398    the fine-textured PAC showing nearly complete uptake of dioxin within 1 hour compared to

399    considerably slower uptake by the coarse texture GAC. These differences could be significant

400    in animal dosing studies but less significant for materials deployed as passive samplers over

401    periods of months to years. Finally, these results could prove useful in the design of large-

402    scale recoverable geosorbents manufactured for contaminant removal.

410

411    **References**

412    Ahn, S., Werner, D., Karapanagioti, H.K., McGlothlin, D.R., Zare, R.N., Luthy, R.G., 2005.

413        Phenanthrene and pyrene sorption and intraparticle diffusion in polyoxymethylene, coke,

414        and activated carbon. Environ. Sci. Technol. 39, (17), 6516-6526.

415    Amarasinghe, B.M.W.P.K., Williams, R.A., 2007. Tea waste as a low cost adsorbent for Cu

416        and Pb removal from wastewater. Chem. Eng. J. 132, 299-309.

417    Balasubramani, A., Rifai, H.S., 2018. Efficacy of carbon-based materials for remediating

418      polychlorinated biphenyls (PCBs) in sediment. Sci. Total Environ. 644, 398-405.

419 Beckingham, B., Ghosh, U., 2011. Field-Scale Reduction of PCB Bioavailability with

420      Activated Carbon Amendment to River Sediments. Environmental Science & Technology

421      45, 10567-10574.

422 Boyd, S.A., Johnston, C.T., Pinnavaia, T.J., Kaminski, N.E., Teppen, B.J., Li, H., Khan, B.,

423      Crawford, R.B., Kovalova, N., Kim, S.S., Shao, H., Gu, C., Kaplan, B.L.F., 2011.

424      Suppression of humoral immune responses by 2,3,7,8-tetrachlorodibenzo-p-dioxin

425      intercalated in smectite clay. Environ. Toxicol. Chem. 30, (12), 2748-2755.

426 Boyd, S.A., Sallach, J.B., Zhang, Y., Crawford, R., Li, H., Johnston, C.T., Teppen, B.J.,

427      Kaminski, N.E., 2017. Sequestration of 2,3,7,8-tetrachlorodibenzo-p-dioxin by activated

428      carbon eliminates bioavailability and the suppression of immune function in mice.

429      Environ. Toxicol. Chem. 36, 2671-2678.

430 Champoux, L., Rail, J.F., Lavoie, R.A., 2017. Polychlorinated dibenzo-p-dioxins,

431      dibenzofurans, and flame retardants in northern gannet (Morus bassanus) eggs from

432      Bonaventure Island, Gulf of St. Lawrence, 1994-2014. Environ. Pollut. 222, 600-608.

433 Charlestra, L., Courtemanch, D.L., Amirbahman, A., Patterson, H., 2008. Semipermeable

434      membrane device (SPMD) for monitoring PCDD and PCDF levels from a paper mill

435      effluent in the Androscoggin River, Maine, USA. Chemosphere 72, 1171-1180.

436 Chai, B.L., Tsoi, T.V., Iwai, S., Liu, C., Fish, J.A., Gu, C., Johnson, T.A., Zylstra, G., Teppen,

437    B.J., Li, H., Hashsham, S.A., Boyd, S.A., Cole, J.R., Tiedje, J.M., 2016. Sphingomonas

438    wittichii strain RW1 genome-wide gene expression shifts in response to dioxins and clay.

439    Plos One 11, (6), 14.

440    Chai, Y.Z., Currie, R.J., Davis, J.W., Wilken, M., Martin, G.D., Fishman, V.N., Ghosh, U.,

441    2012. Effectiveness of activated carbon and biochar in reducing the availability of

442    polychlorinated dibenzo-p-dioxins/dibenzofurans in soils. Environ. Sci. Technol. 46 (2),

443    1035-1043.

444    Chai, Y.Z., Davis, J.W., Wilken, M., Martin, G.D., Mowery, D.M., Ghosh, U., 2011. Role of

445    black carbon in the distribution of polychlorinated dibenzo-p-dioxins/dibenzofurans in

446    aged field-contaminated soils. Chemosphere 82 (5), 639-647.

447    Charnley, G., Doull, J., 2005. Human exposure to dioxins from food, 1999-2002. Food Chem.

448    Toxicol. 43, 671-679.

449    Cho, D.W., Yoon, K., Kwon, E.E., Biswas, J.K., Song, H., 2017. Fabrication of magnetic

450    biochar as a treatment medium for As(V) via pyrolysis of $FeCl_3$-pretreated spent coffee

451    ground. Environ. Pollut. 229, 942-949.

452    Choi, Y.J., Wu, Y.W., Sani, B., Luthy, R.G., Werner, D., Kim, E., 2016. Performance of

453    retrievable activated carbons to treat sediment contaminated with polycyclic aromatic

454    hydrocarbons. J. Hazard. Mater. 320, 359-367.

455    Cornelissen, G., Amstaetter, K., Hauge, A., Schaanning, M., Beylich, B., Gunnarsson, J.S.,

456      Breedveld, G.D., Oen, A.M.P., Eek, E., 2012. Large-scale field study on thin-layer

457      capping of marine PCDD/F-contaminated sediments in Grenlandfjords, Norway:

458      physicochemical effects. Environ. Sci. Technol. 46, 12030-12037.

459      Cornelissen, G., Arp, H.P.H., Pettersen, A., Hauge, A., Breedveld, G.D., 2008a. Assessing

460      PAH and PCB emissions from the relocation of harbour sediments using equilibrium

461      passive samplers. Chemosphere 72, 1581-1587.

462      Cornelissen, G., Gustafsson, O., Bucheli, T.D., Jonker, M.T.O., Koelmans, A.A., Van Noort,

463      P.C.M., 2005. Extensive sorption of organic compounds to black carbon, coal, and

464      kerogen in sediments and soils: Mechanisms and consequences for distribution,

465      bioaccumulation, and biodegradation. Environ. Sci. Technol. 39, 6881-6895.

466      Cornelissen, G., Schaanning, M., Gunnarsson, J.S., Eek, E., 2016. A large-scale field trial of

467      thin-layer capping of PCDD/F-contaminated sediments: sediment-to-water fluxes up to 5

468      years post-amendment. Integr. Environ. Assess. Manag. 12, 216-221.

469      Cornelissen, G., Wiberg, K., Broman, D., Arp, H.P.H., Persson, Y., Sundqvist, K., Jonsson, P.,

470      2008b. Freely dissolved concentrations and sediment-water activity ratios of PCDD/Fs

471      and PCBs in the open Baltic Sea. Environ. Sci. Technol. 42, 8733-8739.

472      Denison, M.S., Fisher, J.M., Whitlock Jr, J.P., 1989. Protein-DNA interactions at recognition

473      sites for the dioxin-Ah receptor complex. J. Biol. Chem. 264, 16478-16482.

474      Denyes, M.J., Rutter, A., Zeeb, B.A., 2013. In situ application of activated carbon and biochar

475  to PCB-contaminated soil and the effects of mixing regime. Environ. Pollut. 182, 201-208.

476 Do, M.H., Phan, N.H., Nguyen, T.D., Thi, T.S.P., Nguyen, V.K., Thi, T.T.V., Thi, K.P.N.,

477  2011. Activated carbon/Fe₃O₄ nanoparticle composite: Fabrication, methyl orange

478  removal and regeneration by hydrogen peroxide. Chemosphere 85, 1269-1276.

479 Eljarrat, E., Monjonell, A., Caixach, J., Rivera, J., 2002. Toxic potency of polychlorinated

480  dibenzo-p-dioxins, polychlorinated dibenzofurans, and polychlorinated biphenyls in food

481  samples from Catalonia (Spain). J. Agric. Food Chem. 50, 1161-1167.

482 Everaert, K., Baeyens, J., 2002. The formation and emission of dioxins in large scale thermal

483  processes. Chemosphere 46, 439-448.

484 Fabietti, G., Biasioli, M., Barberis, R., Ajmone-Marsan, F., 2010. Soil contamination by

485  organic and inorganic pollutants at the regional scale: The case of piedmont, Italy. J. Soil.

486  Sediment. 10, 290-300.

487 Fagervold, S.K., Chai, Y.Z., Davis, J.W., Wilken, M., Cornelissen, G., Ghosh, U., 2010.

488  Bioaccumulation of polychlorinated dibenzo-p-dioxins/dibenzofurans in E. fetida from

489  floodplain soils and the effect of activated carbon amendment. Environ. Sci. Technol. 44

490  (14), 5546-5552.

491 Ferrario, J.B., Byrne, C.J., Cleverly, D.H., 2000. 2,3,7,8-dibenzo-p-dioxins in mined clay

492  products from the united states: Evidence for possible natural origin. Environ. Sci.

493  Technol. 34, 4524-4532.

494     Fiedler, H., 1996. Sources of PCDD/PCDF and impact on the environment. Chemosphere 32,

495         55-64.

496     Ghosh, U., Luthy, R.G., Cornelissen, G., Werner, D., Menzie, C.A., 2011. In situ sorbent

497         amendments: A new direction in contaminated sediment management. Environ. Sci.

498         Technol. 45, 1163-1168.

499     Giles, C.H., Smith, D., Huitson, A., 1974. A general treatment and classification of the solute

500         adsorption isotherm. I. Theoretical. Journal of Colloid and Interface Science 47, 755-765.

501     Gomez-Eyles, J.L., Yupangui, C., Beckingham, B., Riedel, G., Gilmour, C., Ghosh, U., 2013.

502         Evaluation of biochars and activated carbons for in-situ remediation of sediments

503         impacted with organics, mercury, and methylmercury. Environ. Sci. Technol. 47, 13721-

504         13729.

505     Guruge, K.S., Seike, N., Yamanaka, N., Miyazaki, S., 2005. Polychlorinated dibenzo-p-dioxins,

506         -dibenzofurans, and biphenyls in domestic animal food stuff and their fat. Chemosphere

507         58, 883-889.

508     Hale, S.E., Elmquist, M., Brandli, R., Hartnik, T., Jakob, L., Henriksen, T., Werner, D.,

509         Cornelissen, G., 2012. Activated carbon amendment to sequester PAHs in contaminated

510         soil: A lysimeter field trial. Chemosphere 87, 177-184.

511     Han, Z.T., Sani, B., Mrozik, W., Obst, M., Beckingham, B., Karapanagioti, H.K. Werner, D.,

512         2015. Magnetite impregnation effects on the sorbent properties of activated carbons and

513       biochars. Water Res. 70, 394-403.

514    Ho, Y.S., McKay, G., 1999. Pseudo-second order model for sorption processes. Process

515       Biochem. 34, 451-465.

516    Huwe, J.K., 2002. Dioxins in food: a modern agricultural perspective. J. Agric. Food. Chem.

517       50, 1739-1750.

518    Indhu, Z.T., Sani, B., Akkanen, J., Abel, S., Nybom, I., Karapanagioti, H.K., Werner, D., 2015.

519       A critical evaluation of magnetic activated carbon's potential for the remediation of

520       sediment impacted by polycyclic aromatic hydrocarbons. J. Hazard. Mater. 286, 41-47.

521    Johnston, C.T., Khan, B., Barth, E.F., Chattopadhyay, S., Boyd, S.A., 2012. Nature of the

522       interlayer environment in an organoclay optimized for the sequestration of dibenzo-p-

523       dioxin. Environ. Sci. Technol. 46, 9584-9591.

524    Kang, S., Jung, J., Choe, J.K., Ok, Y.S., Choi, Y., 2018. Effect of biochar particle size on

525       hydrophobic organic compound sorption kinetics: Applicability of using representative

526       size. Sci. Total Environ. 619, 410-418.

527    Kaplan, B.L.F., Crawford, R.B., Kovalova, N., Arencibia, A., Kim, S.S., Pinnavaia, T.J., Boyd,

528       S.A., Teppen, B.J., Kaminski, N.E., 2011. TCDD adsorbed on silica as a model for TCDD

529       contaminated soils: Evidence for suppression of humoral immunity in mice. Toxicology

530       282, (3), 82-87.

531    Kim, H.K., Masaki, H., Matsumur, T., Kamei, T., Magara, Y., 2002. Removal efficiency and

532         homologue patterns of dioxins in drinking water treatment. Water Res. 36, 4861-4869.

533    Kulkarni, P.S., Crespo, J.G., Afonso, C.A.M., 2008. Dioxins sources and current remediation

534         technologies-a review. Environ. Int. 34, 139-153.

535    Li, X.M., Peng, P.A., Zhang, S.K., Man, R., Sheng, G.Y., Fu, J.M., 2009. Removal of

536         polychlorinated dibenzo-p-dioxins and polychlorinated dibenzofurans by three coagulants

537         in simulated coagulation processes for drinking water treatment. J. Hazard. Mater. 162,

538         180-185.

539    Louchouarn, P., Seward, S.M., Cornelissen, G., Arp, H.P.H., Yeager, K.M., Brinkmeyer, R.,

540         Santschi, P.H., 2018. Limited mobility of dioxins near San Jacinto super fund site (waste

541         pit) in the Houston Ship Channel, Texas due to strong sediment sorption. Environ. Pollut.

542         238, 988-998.

543    Maier, D., Benisek, M., Blaha, L., Dondero, F., Giesy, J.P., Köhler, H.R., Richter, D., Scheurer,

544         M., Triebskorn, R., 2016. Reduction of dioxin-like toxicity in effluents by additional

545         wastewater treatment and related effects in fish. Ecotoxicol. Environ. Saf. 132, 47-58.

546    Masunaga, S., Yao, Y., Ogura, I., Nakai, S., Kanal, Y., Yamamuro, M., Nakanishi, J., 2001.

547         Identifying sources and mass balance of dioxin pollution in Lake Shinji Basin, Japan.

548         Environ. Sci. Technol. 35, 1967-1973.

549    McKay, G., 2002. Dioxin characterisation, formation and minimisation during municipal solid

550         waste (MSW) incineration: review. Chem. Eng. J. 86, 343-368.

551  Mohan, D., Sarswat, A., Ok, Y.S., Pittman, C.U., 2014. Organic and inorganic contaminants

552  removal from water with biochar, a renewable, low cost and sustainable adsorbent - A

553  critical review. Bioresource Technol. 160, 191-202.

554  Moon, H.B., Yoon, S.P., Jung, R.H., Choi, M., 2008. Wastewater treatment plants (WWTPs)

555  as a source of sediment contamination by toxic organic pollutants and fecal sterols in a

556  semienclosed bay in Korea. Chemosphere 73, 880-889.

557  Oen, A.M.P., Janssen, E.M.L., Cornelissen, G., Breedveld, G.D., Eek, E., Luthy, R.G., 2011.

558  In situ measurement of PCB pore water concentration profiles in activated carbon-

559  amended sediment using passive samplers. Environ. Sci. Technol. 45, 4053-4059.

560  Payne, R.B., Ghosh, U., May, H.D., Marshall, C.W., Sowers, K.R., 2019. A Pilot-Scale Field

561  Study: In Situ Treatment of PCB-Impacted Sediments with Bioamended Activated

562  Carbon. Environmental Science & Technology 53, 2626-2634.

563  Prisciandaroa, M., Piemonteb, V., di Celsoc, G.M., Ronconid, S., Capocelli, M., 2017.

564  Thermodynamic features of dioxins' adsorption. J. Hazard. Mater. 324, 645-652.

565  Sallach, J.B., Crawford, R., Li, H., Johnston, C.T., Teppen, B.J., Kaminski, N.E., Boyd, S.A.,

566  2019. Activated carbons of varying pore structure eliminate the bioavailability of 2,3,7,8-

567  tetrachlorodibenzo-p-dioxin to a mammalian (mouse) model. Sci. Total Environ. 650,

568  2231-2238.

569  Samuelsson, G.S., Raymond, C., Agrenius, S., Schaanning, M., Cornelissen, G., Gunnarsson,

570       J.S., 2017. Response of marine benthic fauna to thin-layer capping with activated carbon

571       in a large-scale field experiment in the Grenland fjords, Norway. Environmental Science

572       and Pollution Research 24, 14218-14233.

573    Shiu, W.Y., Doucette, W., Gobas, F.A.P.C., Andren, A., Mackay, D., 1988. Physical-chemical

574       properties of chlorinated dibenzo-p-dioxins. Environ. Sci. Technol. 22, 651-658.

575    Stedtfeld, R.D., Sallach, J.B., Crawford, R.B., Stedtfeld, T.M., Williams, M.R., Waseem, H.,

576       Johnston, C.T., Li, H., Teppen, B.J., Kaminski, N.E., Boyd, S.A., Tiedje, J.M., Hashsham,

577       S.A., 2017. TCDD administered on activated carbon eliminates bioavailability and

578       subsequent shifts to a key murine gut commensal. Appl. Microbiol. Biotechnol. 101,

579       7409-7415.

580    Tu, Y.J., Chang, C.K., You, C.F., Wang, S.L., 2012. Treatment of complex heavy metal

581       wastewater using a multi-staged ferrite process. J. Hazard. Mater. 209-210, 379-384.

582    Tu, Y.J., Lo, S.C., You, C.F., 2015. Selective and fast recovery of neodymium from seawater

583       by magnetic iron oxide $Fe_3O_4$. Chem. Eng. J. 262, 966-972.

584    Tu, Y.J., You, C.F., Chang, C.K., Wang, S.L., 2013. XANES evidence of arsenate removal

585       from water with magnetic ferrite. J. Environ. Manage. 120, 114-119.

586    USEPA, 1997. Rules of thumb for Superfund remedy selection; EPA 540-R-97-013, OSWER

587       9355.0-69, PB97-963301; U.S. Environmental Protection Agency: Washington, DC.

588    Van den Berg, M., Birnbaum, L., Bosveld, A.T.C., Brunstrom, B., Cook, P., Feeley, M., Giesy,

589     J.P., Hanberg, A., Hasegawa, R., Kennedy, S.W., Kubiak, T., Larsen, J.C., van Leeuwen,

590     F.X.R., Liem, A.K.D., Nolt, C., Peterson, R.E., Poellinger, L., Safe, S., Schrenk, D., Tillitt,

591     D., Tysklind, M., Younes, M., Waern, F., Zacharewski, T., 1998. Toxic equivalency

592     factors (TEFs) for PCBs, PCDDs, PCDFs for humans and wildlife. Environmental Health

593     Perspectives 106, 775-792.

594   WHO, 2010. Exposure to dioxins and dioxin-like substances: a major public health concern.

595     http://www.who.int/ipcs/features/dioxins.pdf.

596   Zhang, Q.L., Lin, Y.C., Chen, X., Gao, N.Y., 2007. A method for preparing ferric activated

597     carbon composites adsorbents to remove arsenic from drinking water. J. Hazard. Mater.

598     148, 671-678.

599   Zhang, S.J., Li, X.Y., Chen, J.P., 2010. Preparation and evaluation of a magnetite-doped

600     activated carbon fiber for enhanced arsenic removal. Carbon 48, 60-67.

601   Zhao, Y.Y., Zhan, J.Y., Liu, G.R., Zheng, M.H., Jin, R., Yang, L.L., Hao, L.W., Wu, X.L.,

602     Zhang, X., Wang, P., 2017. Evaluation of dioxins and dioxin-like compounds from a

603     cement plant using carbide slag from chlor-alkali industry as the major raw material. J.

604     Hazard. Mater. 330, 135-141.

605   Zheng, G.J., Leung, A., Jiao, L.P., 2008. Polychlorinated dibenzo-p-dioxins and diben-

606     zofurans pollution in China: sources, environmental levels and potential human health

607     impacts. Environ. Int. 34, 1050-1061.

608    Zhou, X.J., Buekens, A., Li, X.D., Ni, M.J., Cen, K.F., 2016. Adsorption of polychlorinated

609        dibenzo-p-dioxins/dibenzofurans on activated carbon from hexane. Chemosphere 144,

610        1264-1269.

611

612

613

614    Table titles:

615    Table 1. Selected physical properties of GAC, GAC-$Fe_3O_4$ and PAC.

616    Table 2. Kinetic parameters at different concentration for adsorption of DD by using DSRA

617    and GAC-$Fe_3O_4$ composite.

618

619    Figure Captions

620    Fig. 1. Saturation magnetization of GACs and PAC-$Fe_3O_4$ composites measured by SQUID.

621    Fig. 2. X-ray powder diffraction (XRD) patterns of the GAC-$Fe_3O_4$(B) and PAC-$Fe_3O_4$(A)

622        composites along with reference reflections for magnetite $Fe_3O_4$.

623    Fig. 3. Scanning electron microscopy (SEM) images of (a) DSRA (120X magnitude); (b)

624        DSRA (500X magnitude); (c) DSRA (800X magnitude); (d) GAC-$Fe_3O_4$ composite

625        (50000X magnitude); (e) GAC-$Fe_3O_4$ composite (150000X magnitude); and (f) GAC-

626        $Fe_3O_4$ composite (350000X magnitude).

627      Fig. 4. Batch equilibrium sorption isotherms of dibenzo-p-dioxin (DD) on GAC (black

628            squares) and GAC-$Fe_3O_4$(B) (red circles). Conditions: T=298 K, solution volume=30

629            mL, adsorbent =2.5 mg, contact time=10-48 h.

630      Fig. 5. Sorption kinetics of dibenzo-p-dioxin (DD) uptake by GAC and GAC-$Fe_3O_4$(B) over

631            40 h of contact. Top figure shows results from initial concentration of 0.8 mg/L,

632            middle figure shows results from initial concentration of 0.4 mg/L, and lower figure

633            shows initial concentration of 0.18 mg/L. GAC is represented by black squares and

634            GAC-$Fe_3O_4$(B) is represented by red circles. Conditions: T=298 K, solution

635            volume=30 mL, adsorbent =2.5 mg.

636      Fig. 6. Sorption kinetics of dibenzo-p-dioxin (DD) uptake by GAC, GAC-$Fe_3O_4$(B), PAC and

637            PAC-$Fe_3O_4$(A) over 18 h of contact. PAC is represented by black squares, PAC-

638            $Fe_3O_4$(A) is represented by solid red circles, GAC is represented by open black

639            squares, and GAC-$Fe_3O_4$(B) is represented by open red circles. Conditions: T=298 K,

640            solution volume=30 mL, adsorbent =2.5 mg. Conditions: DD concentration=0.8

641            mg/L, T=298 K, solution volume=30 mL, adsorbent=2.5 mg, contact time=1 h.

642

1    Figure Captions

2    Fig. 1. Saturation magnetization of GACs and PAC-Fe$_3$O$_4$ composites measured by SQUID.

3    Fig. 2. X-ray powder diffraction (XRD) patterns of the GAC-Fe$_3$O$_4$(B) and PAC-Fe$_3$O$_4$(A)

4          composites along with reference reflections for magnetite Fe$_3$O$_4$.

5    Fig. 3. Scanning electron microscopy (SEM) images of (a) DSRA (120X magnitude); (b)

6          DSRA (500X magnitude); (c) DSRA (800X magnitude); (d) GAC-Fe$_3$O$_4$ composite

7          (50000X magnitude); (e) GAC-Fe$_3$O$_4$ composite (150000X magnitude); and (f) GAC-

8          Fe$_3$O$_4$ composite (350000X magnitude).

9    Fig. 4. Batch equilibrium sorption isotherms of dibenzo-p-dioxin (DD) on GAC (black

10          squares) and GAC-Fe$_3$O$_4$(B) (red circles). Conditions: T=298 K, solution volume=30

11          mL, adsorbent =2.5 mg, contact time=10-48 h.

12    Fig. 5. Sorption kinetics of dibenzo-p-dioxin (DD) uptake by GAC and GAC-Fe$_3$O$_4$(B) over

13          40 h of contact. Top figure shows results from initial concentration of 0.8 mg/L,

14          middle figure shows results from initial concentration of 0.4 mg/L, and lower figure

15          shows initial concentration of 0.18 mg/L. GAC is represented by black squares and

16          GAC-Fe$_3$O$_4$(B) is represented by red circles. Conditions: T=298 K, solution

17          volume=30 mL, adsorbent =2.5 mg.

18    Fig. 6. Sorption kinetics of dibenzo-p-dioxin (DD) uptake by GAC, GAC-Fe$_3$O$_4$(B), PAC and

19          PAC-Fe$_3$O$_4$(A) over 18 h of contact. PAC is represented by black squares, PAC-

20        $Fe_3O_4$(A) is represented by solid red circles, GAC is represented by open black

21        squares, and GAC-$Fe_3O_4$(B) is represented by open red circles. Conditions: T=298 K,

22        solution volume=30 mL, adsorbent =2.5 mg. Conditions: DD concentration=0.8

23        mg/L, T=298 K, solution volume=30 mL, adsorbent=2.5 mg, contact time=1 h.
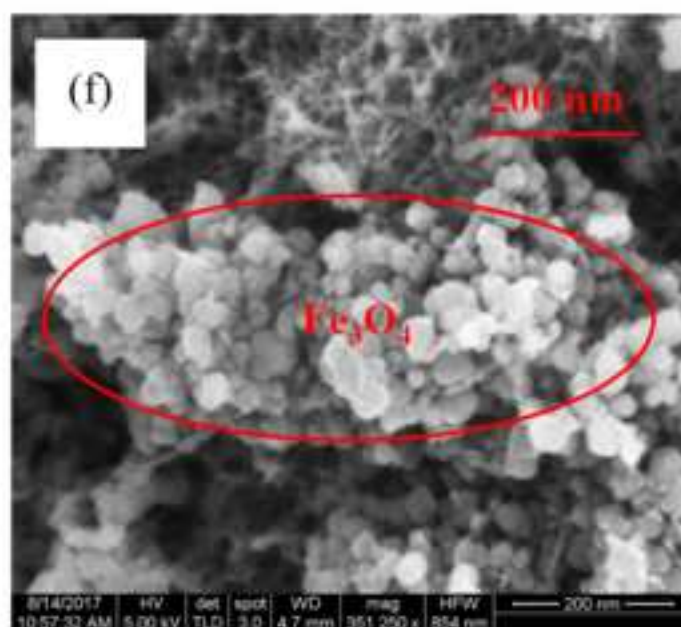
24

25

Figure 1
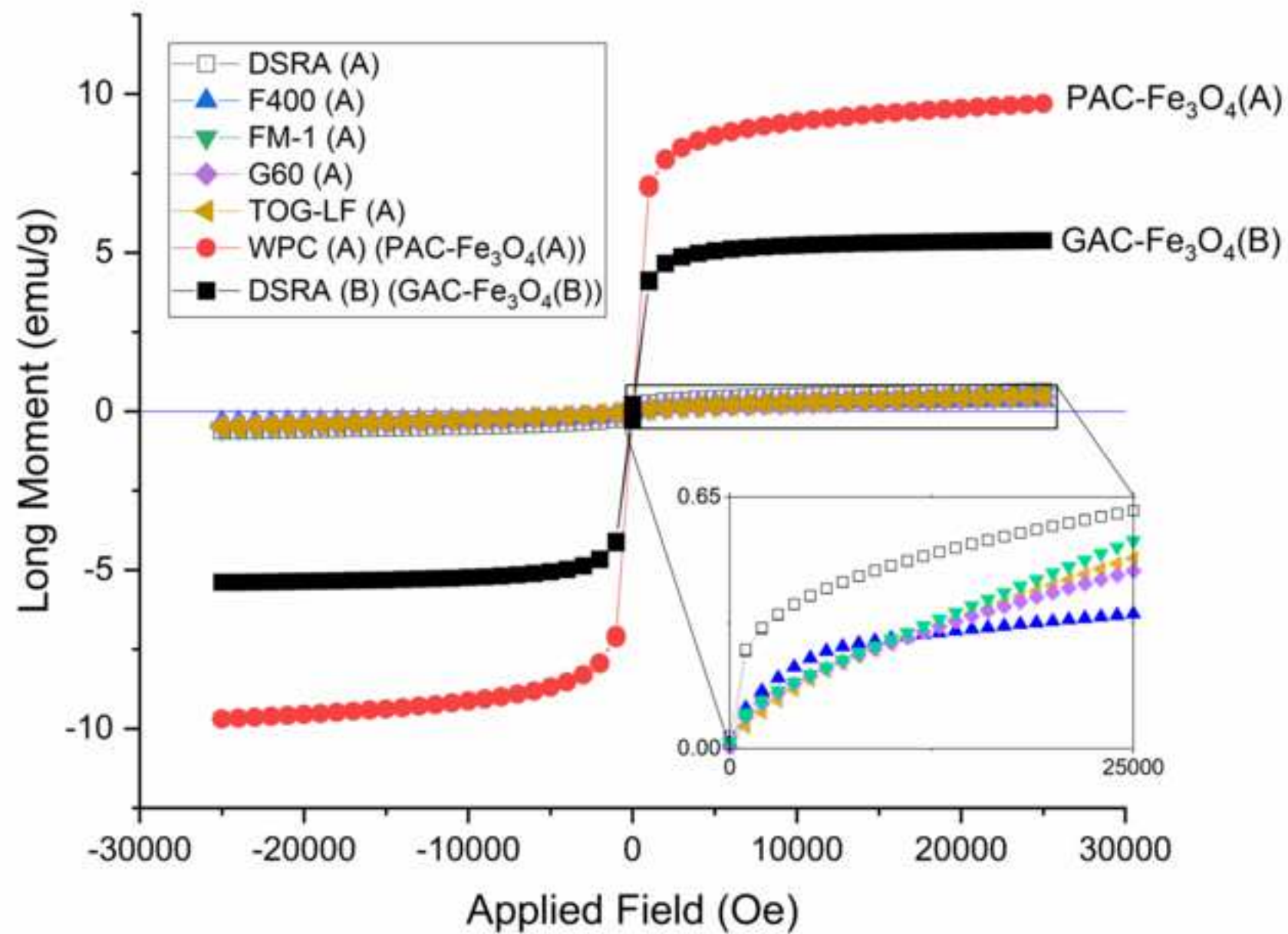
Figure 1
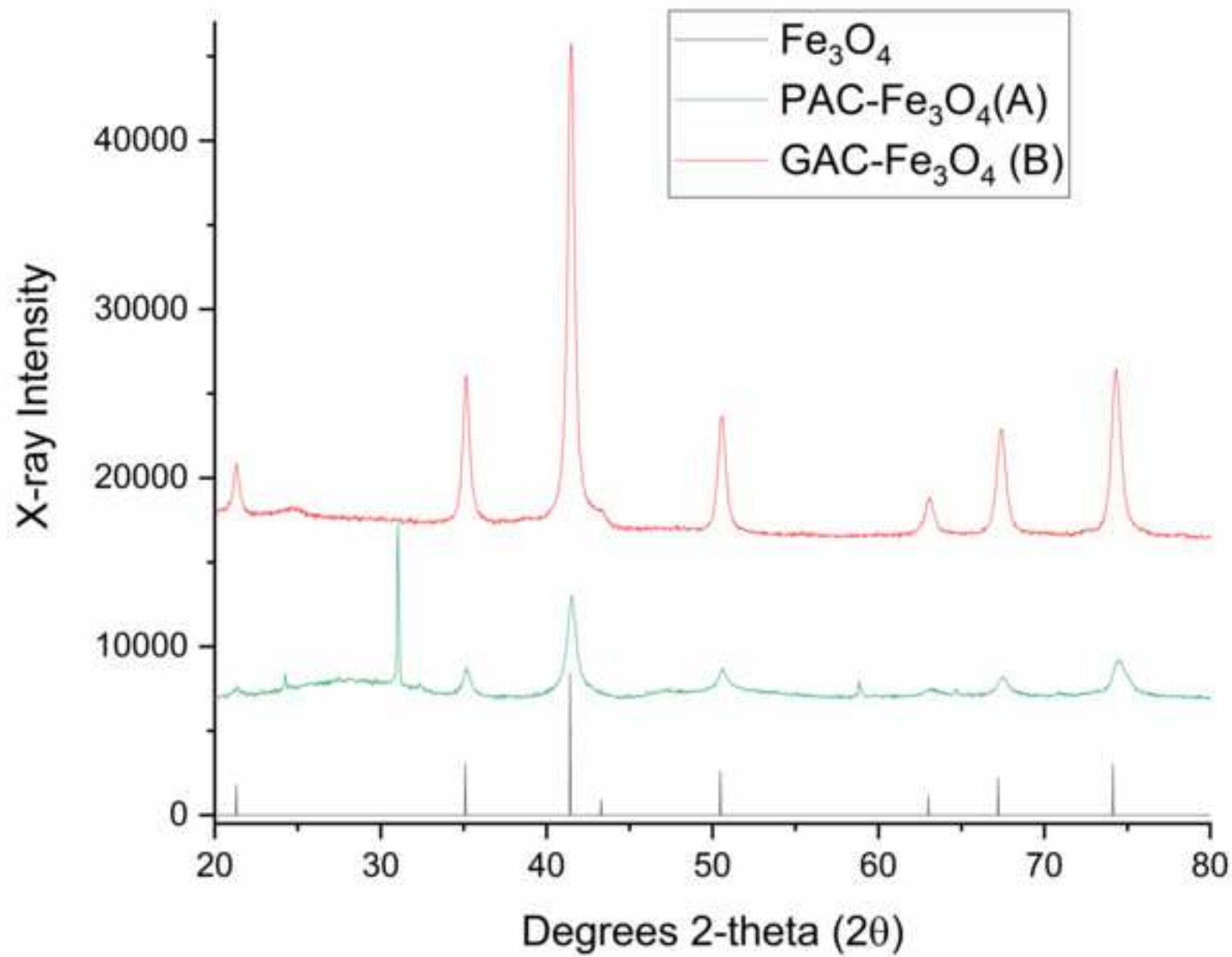
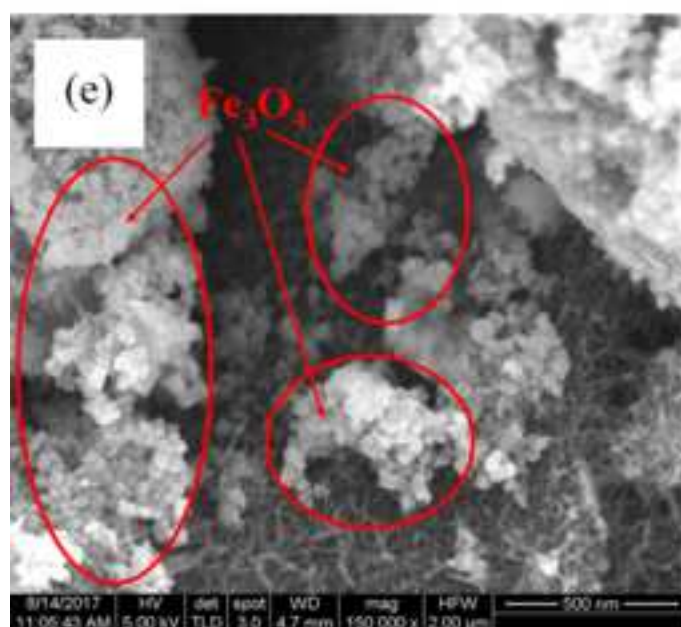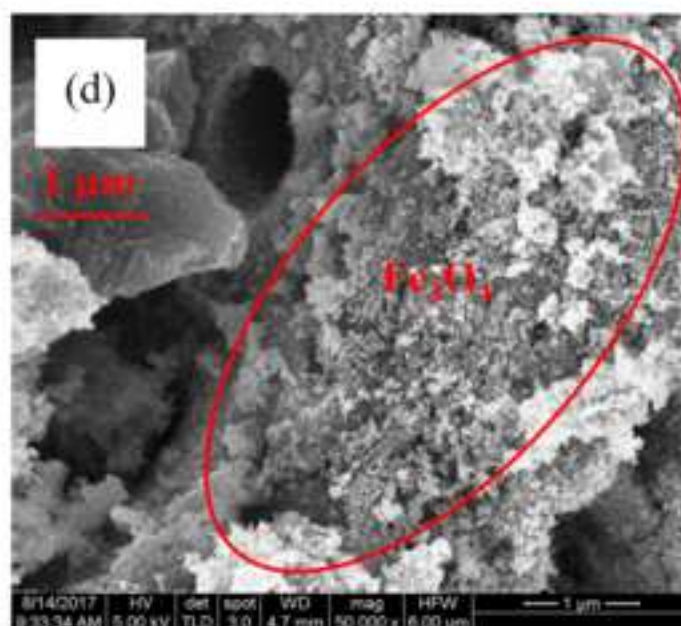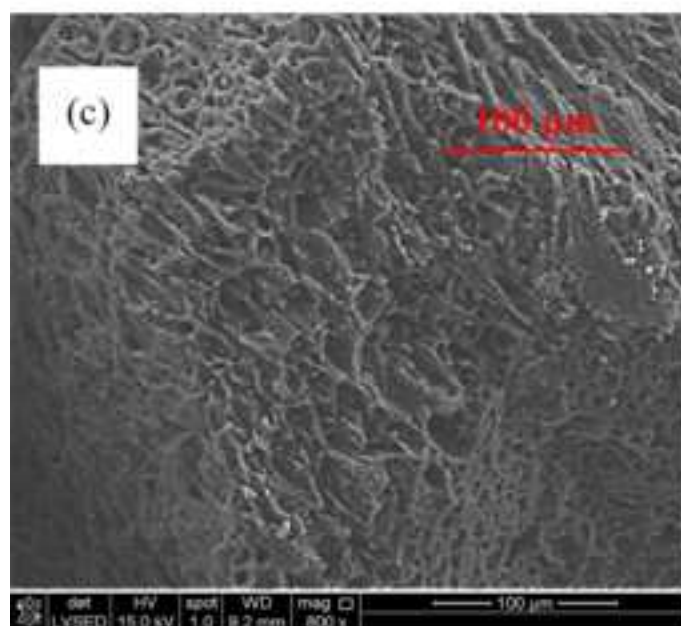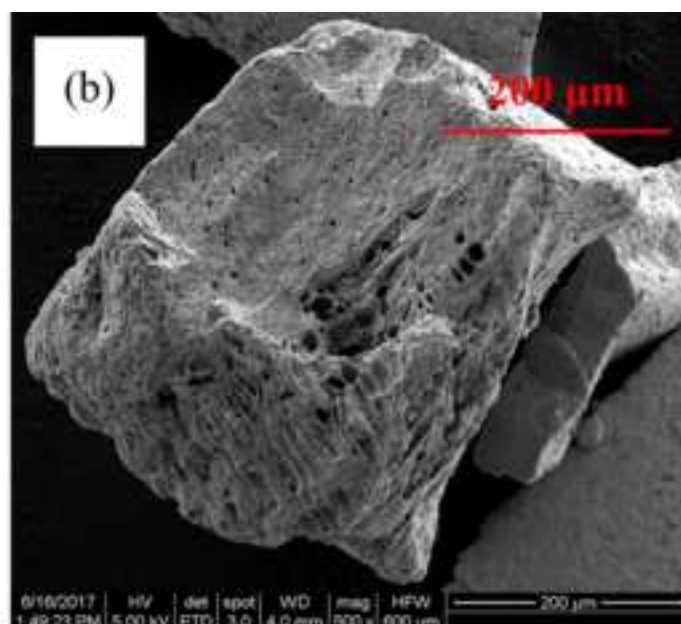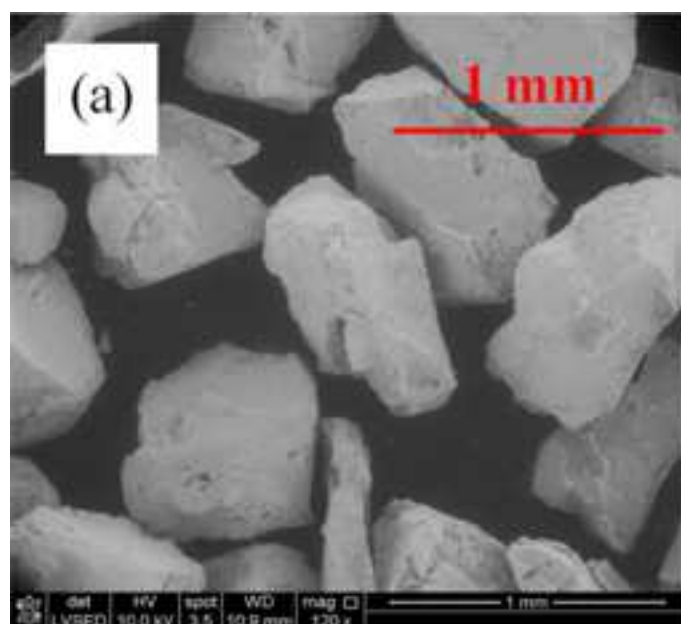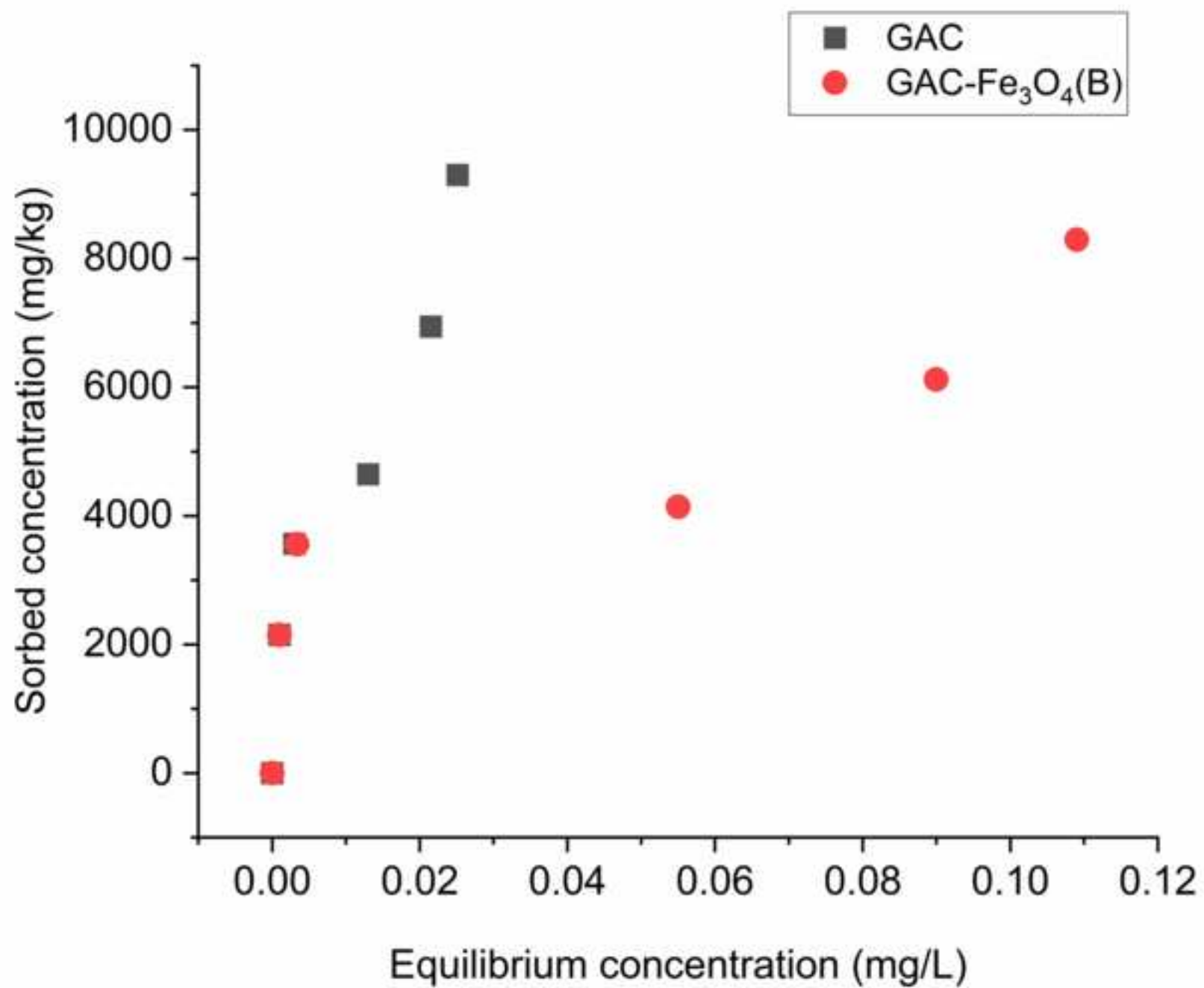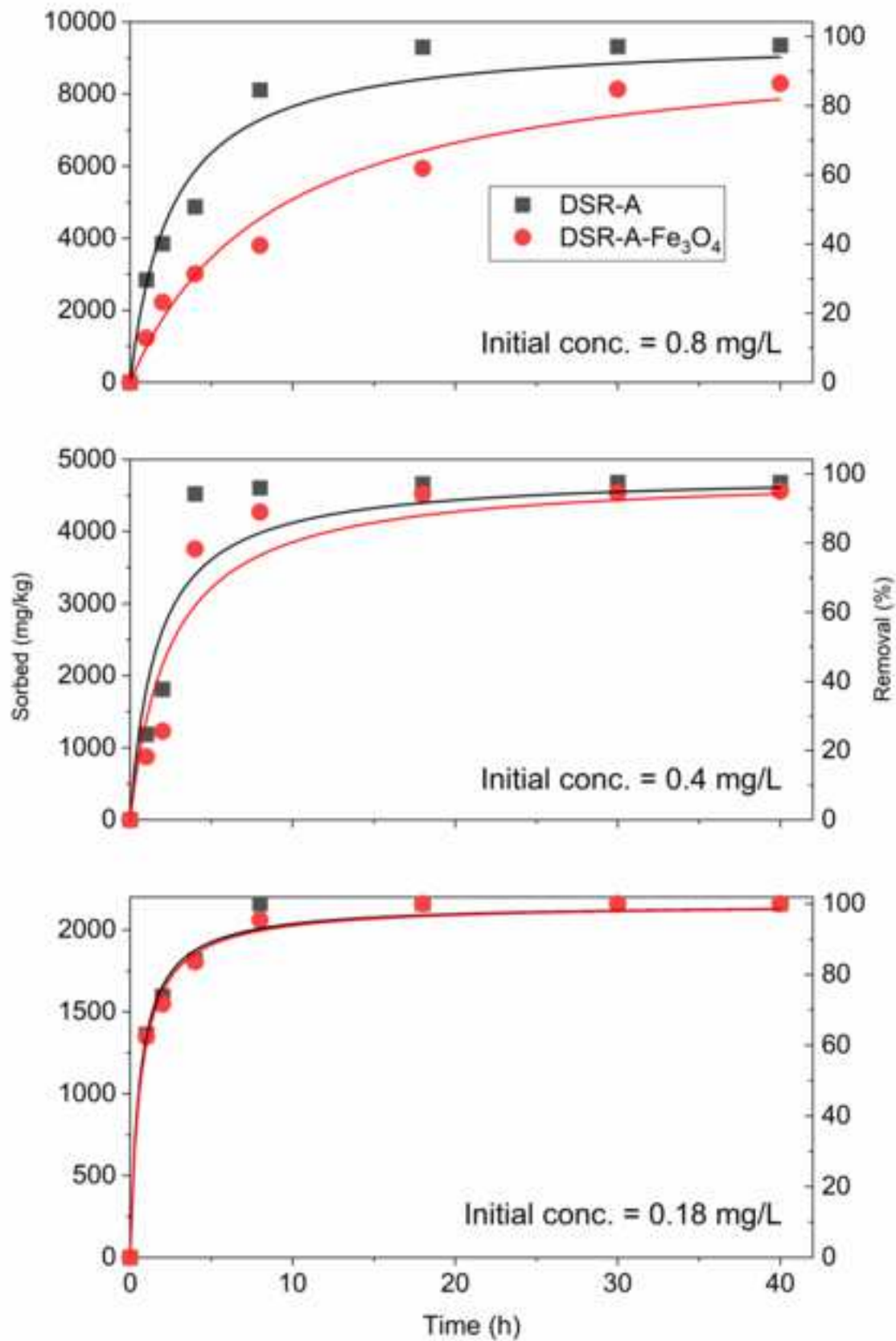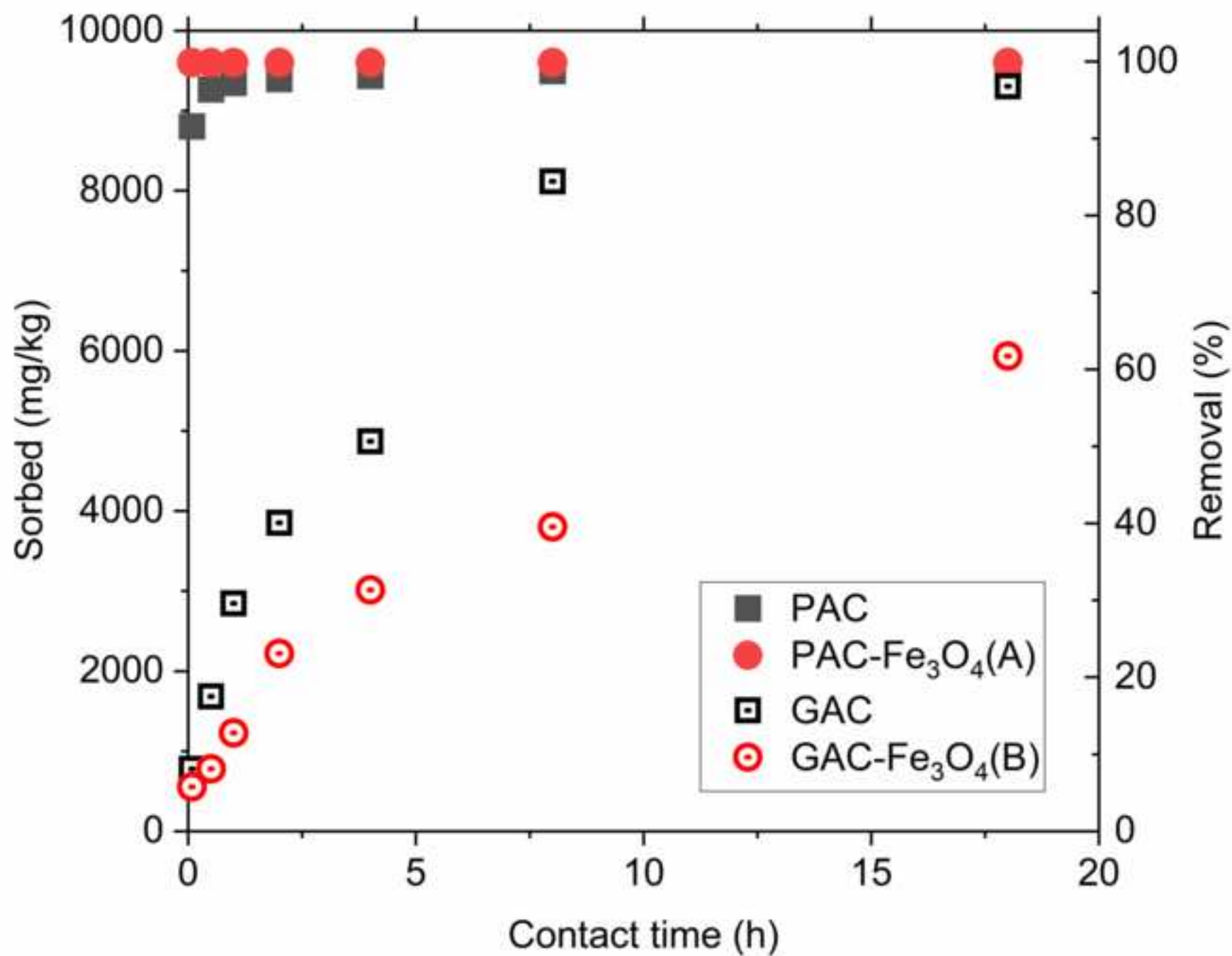Figure 2

Figure 2

Figure 4

Table 1

Table 1. Selected physical properties of the activated carbon materials

| Material | Supplier | Source | Surface Area $(m^2/g)$ | Mesopore vol. g/cc (% of total) | Micropore vol. g/cc (% of total) | [a]Magnetization after Syn. Method A (emu/g) | [b]Magnetization after Syn. Method B (emu/g) |
|---|---|---|---|---|---|---|---|
| G60 | Cabot | Lignite | 987 | 0.38 (57%) | 0.29 (43%) | 0.46 | |
| FM-1 | Cabot | Lignite | 520 | 0.36 (71%) | 0.15 (29%) | 0.54 | |
| TOG-LF | Calgon | Coal | 916 | 0.15 (33%) | 0.30 (67% | 0.49 | |
| F-400 | Calgon | Coal | 1044 | 0.16 (31%) | 0.36 (69%) | 0.35 | |
| WPC (AC) | Calgon | Coconut | 802 | 0.03 (9%) | 0.29 (91%) | 9.7 | |
| DSRA (GAC) | Calgon | Pool Rej. | 822 | 0.11 (22%) | 0.38 (78%) | 0.61 | |
| DSRA-$Fe_3O_4$ | Calgon | Pool Rej. | 633 | 0.06 (18%) | 0.26 (82%) | | 5.38 |

Note:

[a]: Magnetization after $Fe_3O_4$ impregnation at conditions of 338 K and 0.01 M $FeSO_4$.

[b]: Magnetization after $Fe_3O_4$ impregnation at conditions of 298 K and 0.1 M $FeSO_4$.

Table 2

Table 2. The pseudo-second order kinetic model for GAC (DSRA) and GAC-Fe$_3$O$_4$(B)

| | GAC (DSRA) | | | GAC-Fe$_3$O$_4$ (B) | | |
|---|---|---|---|---|---|---|
| | $q_e$ | $k_2$ | Adjusted R Square | $q_e$ | $k_2$ | Adjusted R Square |
| 0.18 mg/L | 2160 | 7.62E-04 | 0.990 | 2160 | 7.02E-04 | 0.994 |
| 0.4 mg/L | 4800 | 1.26E-04 | 0.893 | 4800 | 8.47E-05 | 0.916 |
| 0.8 mg/L | 9600 | 4.10E-05 | 0.967 | 9600 | 1.17E-05 | 0.973 |